CHAPTER VI

PRESSURE STUDIES ON 4-n-ALKOXYPHENYL-4'-(4"-NITROBENZOYLOXY) BENZOATE HOMOLOGOUS SERIES: PRESSURE INDUCED TRIPLY REENTRANT BEHAVIOUR IN A SINGLE COMPONENT SYSTEM

6.1 INTRODUCTION

As a rule, the sequence of transitions exhibited by a polymesomorphic material as it is cooled from the isotropic phase is as follows:

Isotropic → Nematic → Smectic A → Solid

A remarkable departure from this sequence was discovered by Cladis[1] in the binary system of n-p-cyanobenzylidene-p'-octyloxyaniline (CBOOA) and p-[p'-hexyloxybenzylidene)amino] benzonitrile (HBAB). She found that for some concentrations, the smectic A to nematic (A-N) transition was multivalued, i.e., when the temperature was varied at a fixed concentration, the mixture exhibited a nematic phase at higher as well as lower temperatures with respect to the smectic A phase. This phenomenon designated as "reentrance" (the lower temperature nematic being the reentrant nematic phase) in analogy with similar phenomena which are already known in condensed matter physics.[2-5] Two years later Cladis et al.[6] observed a similar behaviour for a single component system at high pressure. Soon

afterwards pure compounds (single component systems) exhibiting the reentrant nematic phase at atmospheric pressure were synthesized and this has led to a large number of studies.

The compounds in which the reentrant nematic behaviour was reported for the first time at atmospheric pressure were 4-n-octyloxy-benzoyloxy-4'-cyanostilbene (T_8)[7] synthesized by the Bordeaux group and trans-p-n-decyloxy-a-methyl-p'-cyanophenyl cinnamate (10OMCPC)[8] synthesized at Bangalore. Almost simultaneously similar compounds were also synthesized by the Berlin group.[9] The structure and the transition temperatures of these compounds are given in Fig. 6.1.. It was also observed that in the case of materials synthesized by the Bordeaux and Berlin groups, there exists not only a reentrant nematic phase but also a reentrant smectic phase, i.e., both T_8 and 4-nonyloxybenzoyloxy-4'-cyanoazobenzene (9OBCAB) show the sequence :

Nematic → Smectic A → Nematic → Smectic A

X-ray studies[10,11] showed that the higher temperature smectic A phase is in fact of the partially bilayer (A_d) type ($\frac{d}{\ell} > 1$) while the lower temperature smectic phase is of the monolayer (A_1) type ($\frac{d}{\ell} \sim 1$ The synthesis of these compounds has led to a lot of interest in the search for other materials which are likely to exhibit reentrant behaviour. (For a recent review of the materials exhibit-

1. 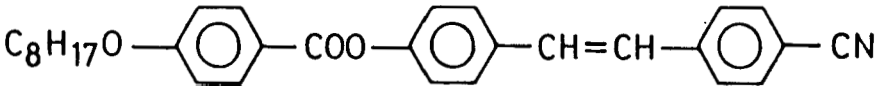

4 – n – octyloxybenzoyloxy – 4′–cyano stilbene (T_8)[7]

2. 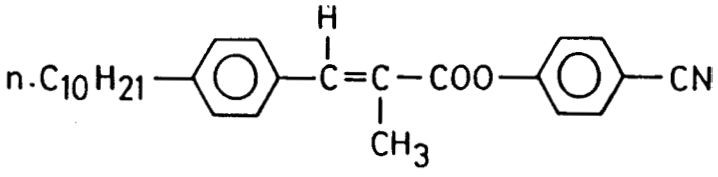

trans–p–n–decyloxy – α–methyl – p′–cyanophenyl cinnamate[8]

(10.O.MCPC)

3. 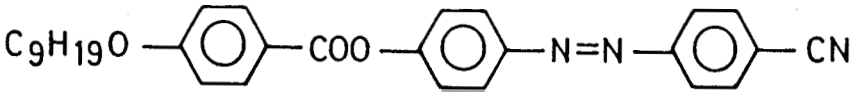

4–nonyloxybenzoyloxy – 4′ – cyanoazobenzene[9]

(9.O.BCAB)

Figure 6.1

Chemical structures of the compounds exhibiting reentrant nematic phase at atmospheric pressure.

ing the reentrant nematic phase see Ref. 12). It is now recognized that reentrant nematic behaviour is generally found in compounds which have the following molecular structure :

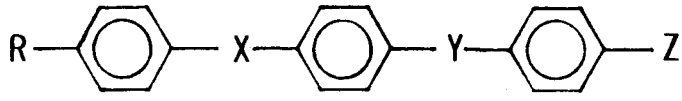

Here R stands for the alkyl or alkoxy group, X and Y denote the bridging groups, while Z denotes the strongly polar group (CN or NO_2). For Z = CN (i.e., when the terminal polar group is a cyano group), the reentrant nematic phase is observed when the longitudinal component of the dipole of X is additive with respect to the cyano end group. The dipolar direction of Y does not seem to have any bearing on the occurrence of the reentrant nematic phase. On the other hand, when the terminal polar group is a nitro group, reentrant nematic behaviour is seen only when the longitudinal components of both X and Y are in opposition to the direction of the terminal nitro group. Such a disposition of the dipoles also leads to a variety of smectic A polymorphism which has been discussed in Chapter III. In this chapter we shall be interested only in the reentrant behaviour of such materials.

We saw that the necessary condition for the appearance of reentrant nematic phase is that the constituent molecules should possess a strongly polar cyano or nitro end group. (Exceptions to this rule has been observed very recently.[13] We shall be discussing these cases in Chapter VII.) Particular mention can be made

of the fact that a material with a terminally nitro end group has in fact shown the richest variety of smectic A phases known so far in any liquid crystalline system. This material, namely, 4-n-nonyloxyphenyl-4'-(4"-nitrobenzoyloxy) benzoate (DB9.O.NO_2) which was first synthesized by the Bordeaux Group[14] exhibits the following sequence of transitions:

$$I \rightarrow N \rightarrow A_d \rightarrow N_{re} \rightarrow A_{d(re)} \rightarrow N_{re} \rightarrow A_1 \rightarrow \tilde{C} \rightarrow C_2 \rightarrow K$$

The same material which was subsequently synthesized by Dr. V. Surendranath in our laboratory showed an additional A phase, viz., A_2-phase between the $\tilde{C}$ and C_2 phases, probably because the material was of greater purity. (This will be discussed in detail later.)

Since the nematic phase reenters twice and A_d once this material has been referred to as a triply reentrant mesogenic system. It should also be mentioned that the occurrence of reentrant polymorphism appears to be extremely sensitive to changes in molecular length. It has been observed that although DB9.O.NO_2 shows such a rich variety of reentrant phase transitions (3 nematic and 3 smectic A phases), its lower as well as higher homologues shows only a single nematic - smectic A transition. It is of considerable interest to know how these phase transitions behave at high pressure. For this purpose, we have carried out a pressure study of the seventh to tenth homologues of the DBn.O.NO_2 series. In addition, we have

carried out optical and X-ray studies on DB9.O.NO_2. The results of these investigations are presented in this chapter.

6.2 MATERIALS

The chemical structure of the 4-n-alkoxypheyl-4'-(4"-nitrobenzoyloxy)benzoate (DBn.O.NO_2) homologous series is given in Fig. 6.2, while the transition temperatures of the compounds studied, i.e., n = 7 to 10, are given in Table 6.1. As already mentioned, DB9.O.NO_2 has been synthesized in our laboratory by Dr. V. Surendranath, while the others were kindly given to us by Prof. G.Heppke, Technical University of Berlin. Table 6.1 shows that the phase sequences are highly sensitive to changes in the chain length.

6.3 EXPERIMENTAL

High pressure studies were conducted using an optical cell with sapphire windows. The sample was isolated from the pressure transmitting fluid by Fluran. The transition temperatures were determined using optical transmission technique which has already been described in Chapter II. Pressure was measured using a Heise gauge with a precision of ±1.5 bar andtemperature to ± 25 mK.

X-ray studies were conducted using the photographic set up described in Chapter II. The sample was taken in a Lindemann glass capillary of diameter 0.5 mm whose ends are then sealed. It was

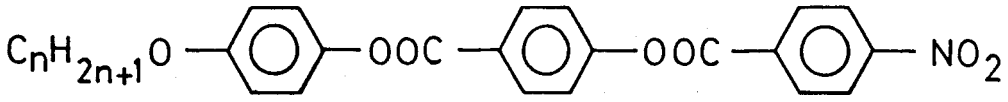

(n = 7, 8, 9 and 10)

4 - n - alkoxyphenyl - 4^{I} - (4^{II} - nitrobenzoyloxy) benzoate

($DBn{\cdot}O{\cdot}NO_2$).

Figure 6.2

***The** molecular structure of the 4-n-alhoxyphenyl nitrobenzoyloxy benzoate ($DBn.O.NO_2$) homologous series.*

Table 6.1

Transition temperatures (in °C) at atmospheric pressure of DBn.O.NO_2 homologous series for n = 7,8,9 and 10.

Compound	I	N	A_d	N_{re}	$A_{d(re)}$	N_{re}	A_1	$\tilde{C}$	A_2	C_2	K
DB7.O.NO_2	. 230.5 .	-	-	-	-	128.8 .	101.8 .	-	-	85.2 .	
DB8.O.NO_2	227	-	-	-	-	130	109	-	-	86.4 .	
DB9.O.NO_2	. 224 .	195 .	156 .	138.5 .	124 .	121.5 .	119 .	100 .	96 .	88.2 .	
DB10.O.NO_2	. 220 .	210.8 .	-	-	-	-	119 .	-	107.4 .	89 .	

. indicates that the phase exists

- represents the phase is absent.

cooled from the nematic phase at very slow rate so as to orient the sample using the magnetic field (~ 0.5 T). Temperature was maintained during any exposure (typically, 15-20 minutes) to a constancy of 0.1°C or better. The relative accuracy in the determination of the layer spacing is reckoned to be ± 0.1 Å.

6.4 RESULTS AND DISCUSSION

The scheme of presentation of the results is as follows. The high pressure studies on DB7.O.NO_2 and DB8.O.NO_2 are presented followed by a detailed study on DB9.O.NO_2 which includes optical microscopy, X-ray and 'high pressure. This is then followed by the high pressure studies on DB.10.O.NO_2. Finally, the temperature-concentration diagram for the binary system of DB10.O.NO_2 and DB8.O.NO_2 is presented along with the high pressure studies on a 57 mol% mixture of DB10.O.NO_2 in DB8.O.NO_2.

Pressure Studies

6.4.1 DB7.O.NO_2 : The pressure-temperature (P-T) diagram of this compound is shown in Fig. 6.3. (It should be mentioned that for none of the four compounds as well for the 57 mol % mixture investigated was it possible to follow the nematic-isotropic (N-I) transition as a function of pressure because of the high T_{NI} values even at atmospheric pressure.) It is seen that both A_1 - N and $\tilde{C}$ - A_1 phase boundaries are linear, but with different slopes - the dT/dP value

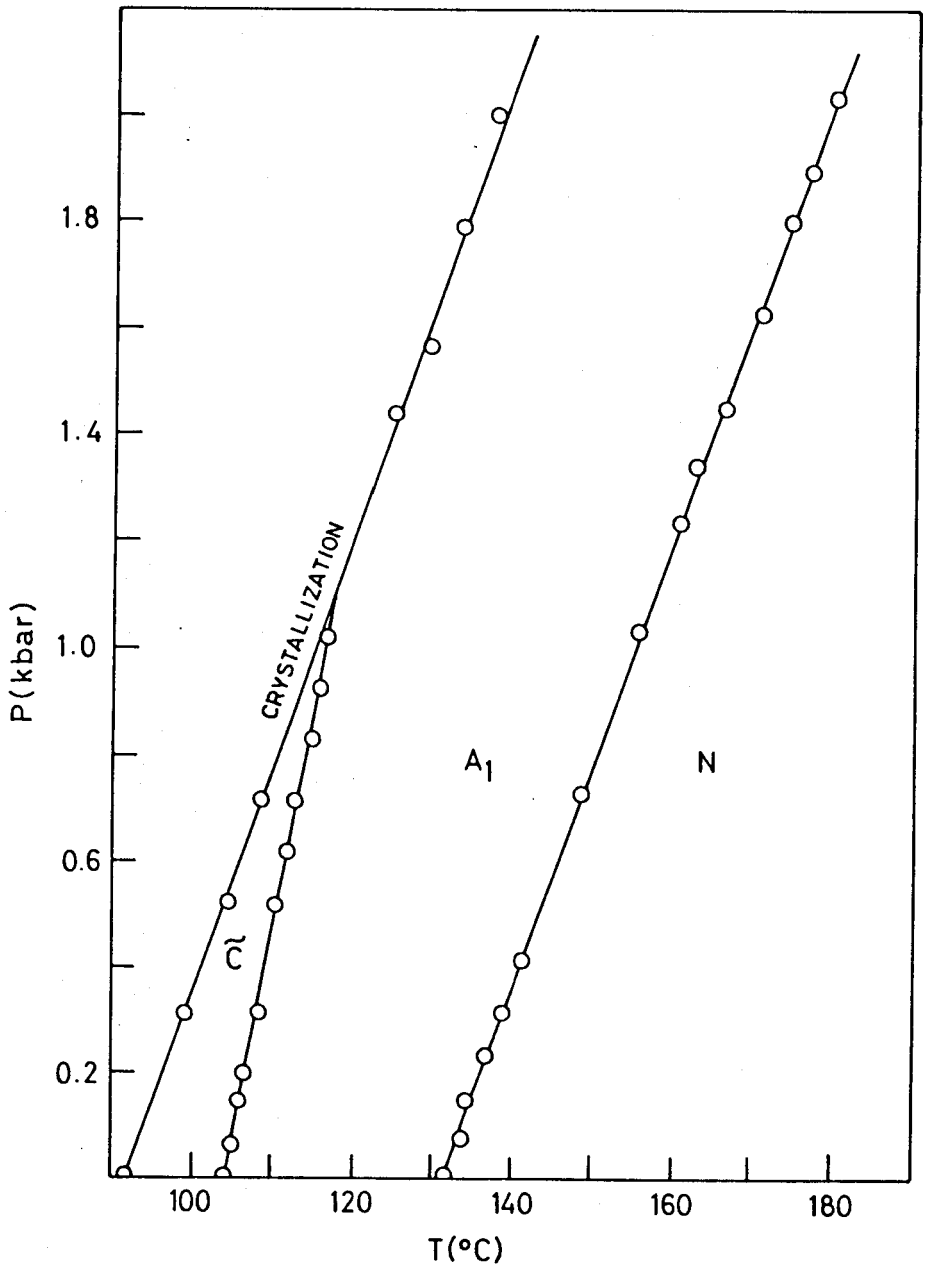

Figure 6.3

Pressure-temperature diagram of DB7.O.NO_2.

for the A_1 - N boundary is 24.3 °C/kbar while that for the $\tilde{C}$ - A_1 line is 12.6 °C/kbar. Consequently, with increasing pressure the range of A_1 increases while that of $\tilde{C}$ decreases until at a pressure of 1.12 kbar the $\tilde{C}$ phase is suppressed because of the intersection of the crystallization line with the $\tilde{C}$ - A_1 boundary. The lack of curvature of the A_1 - N boundary clearly rules out the existence of a reentrant nematic phase.

6.4.2. DB8.O.NO_2 : Fig. 6.4 shows the pressure-temperature diagram of this compound. It is very much similar to that of the lower member discussed earlier. The only difference is that the difference in dT/dP values for $\tilde{C}$ - A_1 and A_1 - N boundaries (16.1 and 26.3 °C/ kbar) are less than that in the case of DB7.O.NO_2. As a result, the $\tilde{C}$ phase is seen till higher pressures in DB8.O.NO_2, although it ultimately gets suppressed at - 2.54 kbar. Here again there is no evidence of a reentrant nematic up to 2.6 kbar, the maximum pressure studied. Thus pressure does not induce any new phases in either DB7.O.NO_2 or DB8.O.NO_2.

6.4.3. DB9.O.NO_2: As mentioned earlier this compound was synthesized by Dr. V.Surendranath in our laboratory, and perhaps because of greater purity of the material, an addition1 phase, viz., the A_2 phase, not reported earlier,[14] was identified between $\tilde{C}$ and C_2 in our studies. This is confirmed by our microscopic, X-ray

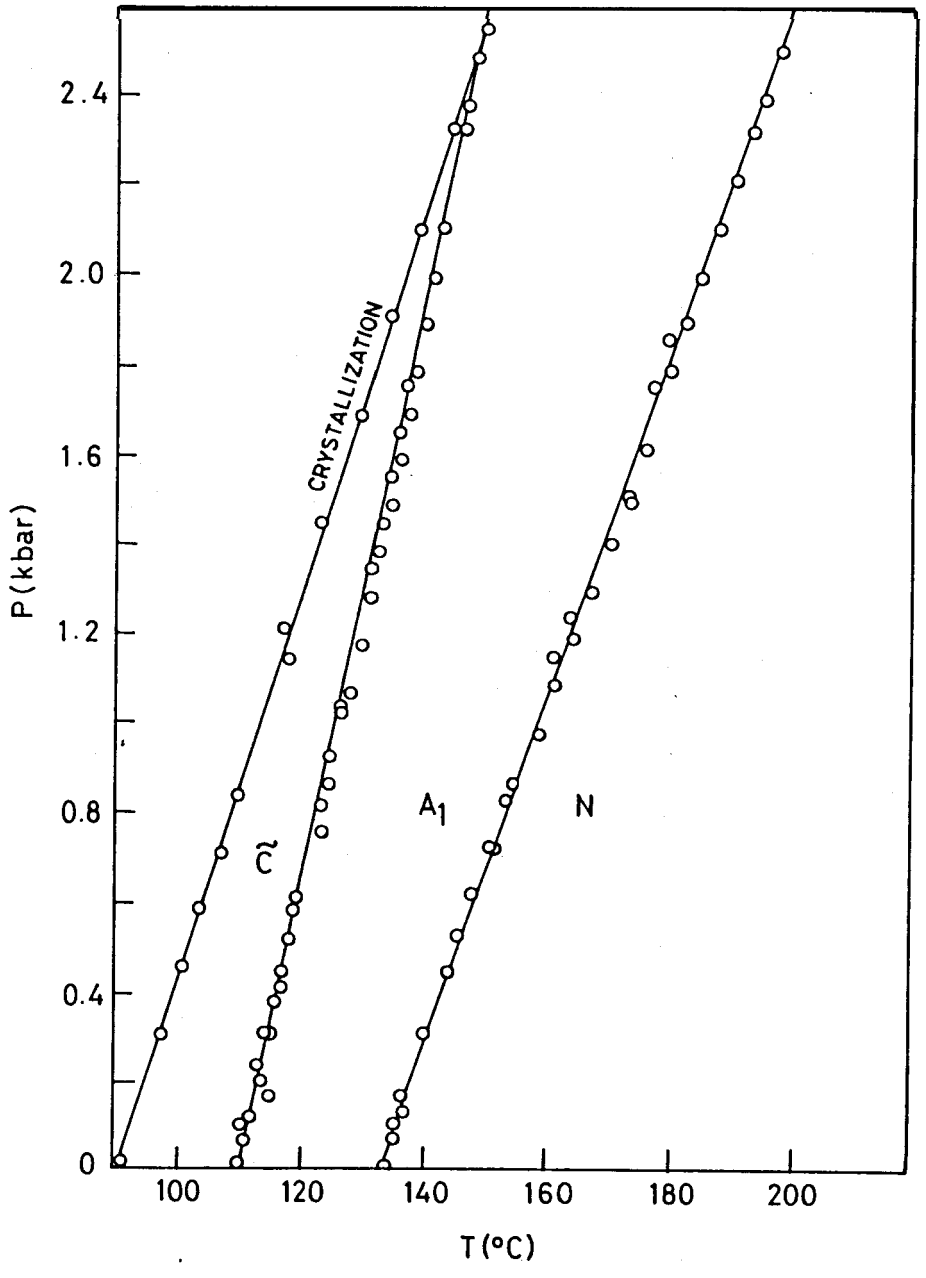

Figure 6.4

P - T diagram of $DBS.O.NO_2$.

and high pressure studies. We shall first present the results of our optical microscopic studies.

a) Microscopic studies on DB9.O.NO$_2$: These studies were carried out using a Leitz Orthoplan polarizing microscope and a Mettler hot stage (FP82) with a temperature controller (FP800). Figures 6.5a-c show the textures in the $\tilde{C}$, A_2 and C_2 phases respectively evolved on cooling the focal conic texture of the A_1 phase. The changes are clearly seen. These changes are seen more clearly when a homeotropically aligned A_1 phase is cooled (Fig. 6.5d-f). Under these conditions $\tilde{C}$ phase shows its characteristic texture[15] (Fig. 6.5d) which disappears on the formation of the A_2 phase - a dark field being seen between crossed polars (Fig. 6.5e). On going over to the C_2 phase a typical Schlieren texture is seen (Fig. 6.5f). Thus the A_2 phase can be clearly distinguished from the $\tilde{C}$ and C_2 phases by microscopic studies. It should however be mentioned that the existence of A_2 as well as the second (or lower temperature) N_{re} phase seemed to be strongly dependent on the purity of the sample; impure samples failed to show these phases. The same effect was seen in samples heated repeatedly to high temperatures.

b) X-ray studies. The thermal variation of the layer thickness (d) in the different phases of DB9.O.NO$_2$ is shown in Fig. 6.6. Starting from the higher temperature A_d phase, with decrease in temperature d shows a continuous increase, d/ℓ increasing

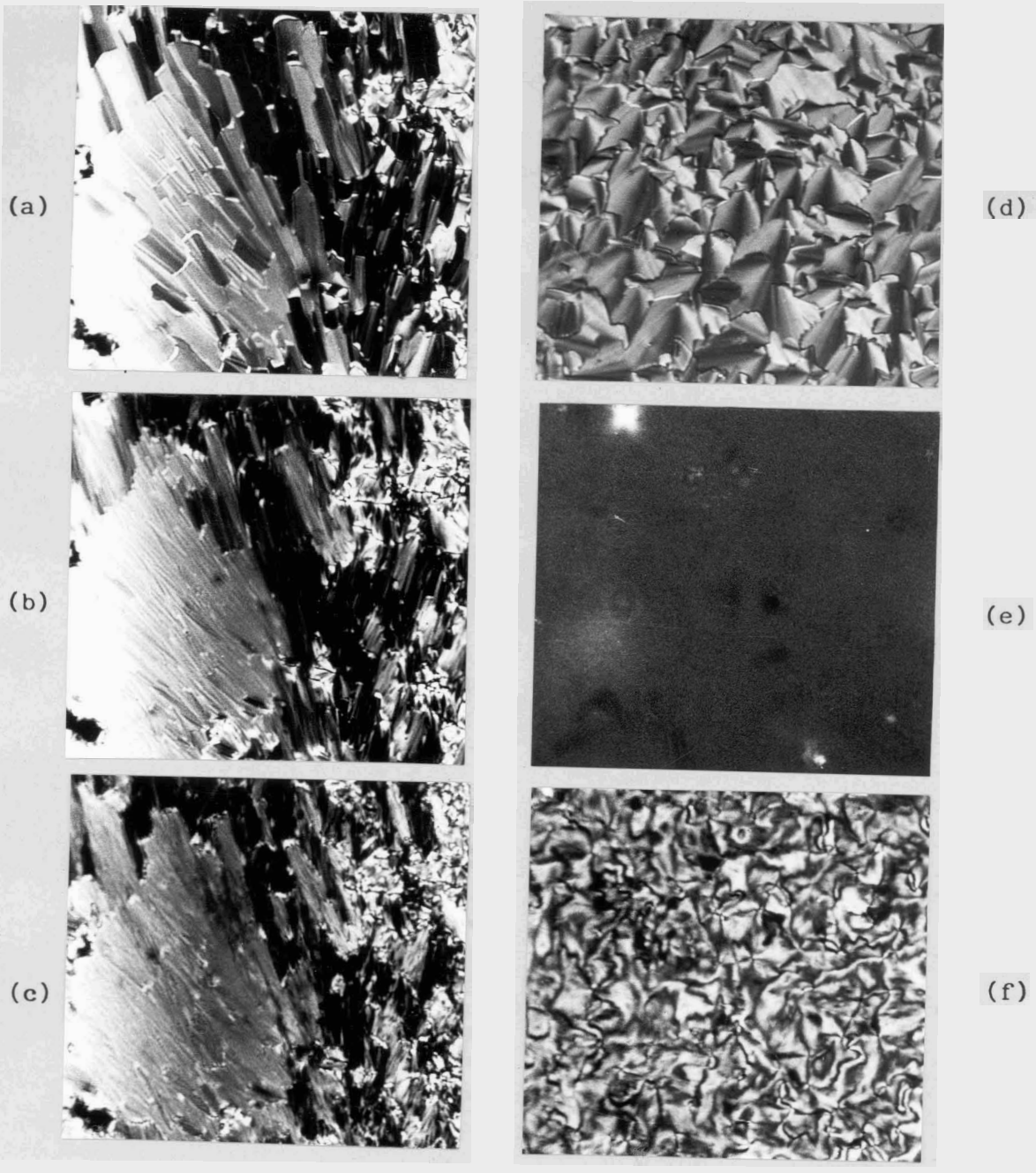

Figure 6.5

Optical textures in the $\tilde{C}$, A_2 and C_2 phases of DB9.O.NO$_2$; crossed polarizers x250. a-c: textures obtained on cooling a focal conic region of the A_1 phase, (a) 103°C. $\tilde{C}$ phase, (b) 98°C, A_2 phase, (c) 97°C, C_2 phase; d-f: textures evolved on cooling a homeotropic domain of the A_1 phase, (d) 114.6°C, $\tilde{C}$ phase, (e) 98°C, A_2 phase, (f) 92.8°C, C_2 phase.

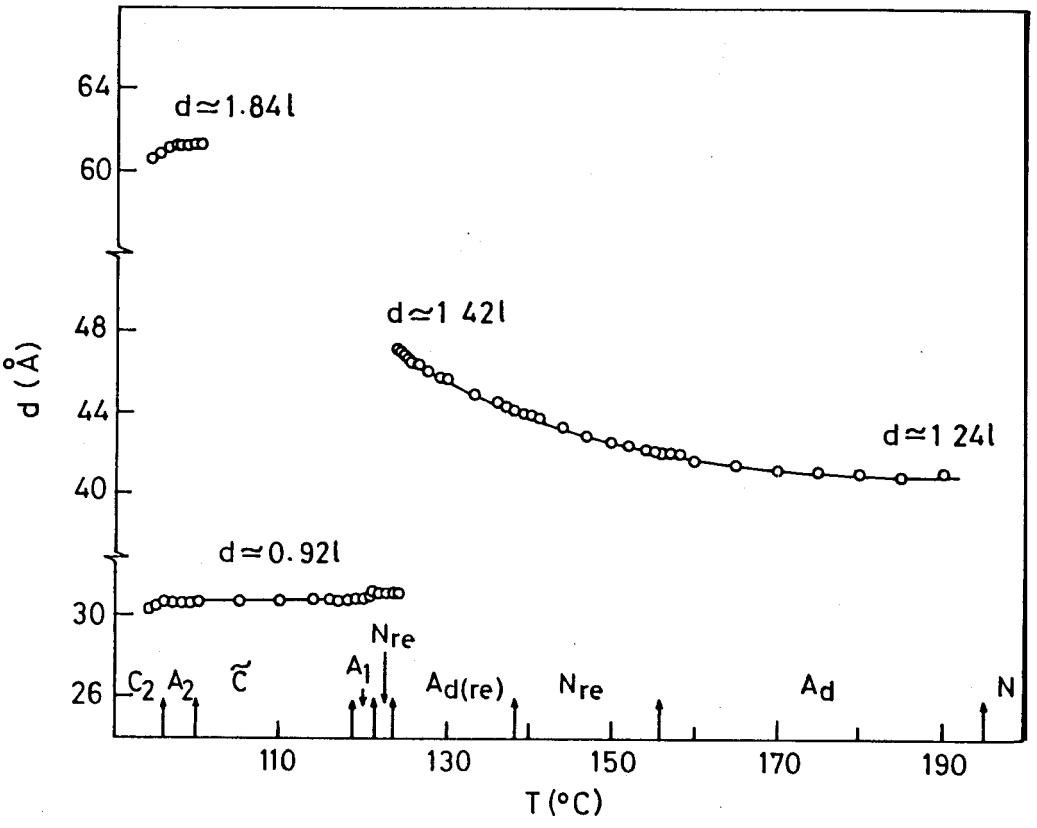

Figure 6.6

Temperature valriation of the layer spacing (d) in the different phases of DB9.O.NO$_2$. The arrows in the figure represent the transition temperatures.

from 1.24 at the highest temperature to about 1.42 just before the onset of the A_1 phase. This increasing trend is seen right through the $A_d - N_{re}$ and $N_{re} - A_{d(re)}$ transitions. Essentially a similar behaviour was seen earlier also.[16] It should also be mentioned that the diffraction spots in the N_{re} phase was as sharp as those in the A_d phase signifying the existence of strong smectic-like local ordering in this phase. As the second or lowest temperature reentrant nematic phase (which exists between $A_{d(re)}$ and A_1 phases) is approached both q_0' as well as $2q_0$ reflections corresponding to the $A_{d(re)}$ and A_1 phases were observed showing thereby the existence of two types of short range ordering in this phase.As the temperature is lowered the intensity of q_0' decreases with an accompanying increase in the intensity of $2q_0$. At the second reentrant nematic-A_1 transition the q_0' spots become diffuse. Also the diffuse q_0' spots progressively show a large spread along X-direction and finally a constriction is seen at the middle (see Fig. 6.7). Thus we observed off Z-axis fluctuations in the A_1 phase. (It must be mentioned here that Hardouin and Levelut[17] have made similar observtions in T_8.) These diffuse off Z-axis spots can be viewed as a precursor to $\tilde{C}$ phase. It is relevant to recall that recently Wang and Lubensky[18] have predicted the diffuse scattering that is expected in the A_1 phase on approaching different types of phases. According to them, on approaching the A_2 phase a diffuse spot centered around q_0 should be seen. But if the approaching

Figure 6.7

Photograph showing the diffuse off Z-axis Xray spots in the A, phase (121°C) along with the condensed $2q_0$ spots.

phase is $\tilde{A}$, then the X-ray pattern is expected to show a diffuse ring centred around q_0. On the other hand on approaching the $\tilde{C}$ phase, two diffuse rings spaced on either side of q_0 are expected. Finally, on approaching an incommensurate smectic A phase, a 'double spot pattern' consisting of condensed $2q_0$' diffuse spots corresponding to q_0' and a combination of $2q_0$ and q_0' is predicted. On the other hand it can also exhibit the coexistence of the diffuse spots on either side of the diffuse ring at q_0 corresponding to the competition between $\tilde{A}$ and incommensurate phases.

In our studies on DB9.O.NO_2, we see $\tilde{C}$-like fluctuations in the A_1 phase. On further reduction of temperature, the typical X-ray pattern of the $\tilde{C}$ or ribbon phase[19] is seen (see Fig. 6.8). The characteristic feature of this pattern is the presence of two off Z-axis spots which have asymmetric intensity. It can be recalled from the work of Hardouin et al.[19] that there can be an undulation of the layers. They have given the model of the $\tilde{C}$ phase, according to which this phase can be described as a regular stacking of bimolecular tilted regions with periodic stacking faults.

Finally, on cooling the $\tilde{C}$ phase further we observed the sudden condensation of the spot at q_0 in addition to the condensed $2q_0$. This corresponds to the A_2 phase. Thus we have characterised the A phase seen between $\tilde{C}$ and C_2 phases as the smectic bilayer (A_2) phase. In the A_2 phase a temperature independent layer spacing

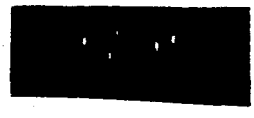

Figure 6.8

Photograph showing the Xray diffraction spot for the $\tilde{C}$ *phase (110°C).*

is seen but on going over to C_2 phase there is a decrease in layer spacing due to the tilting of the bilayer structure.

Recently Fontes et al.[20] have performed high resolution X-ray scattering studies on DB9.O.NO$_2$. Their results are similar to ours. They also carried out detailed studies in the $\tilde{C}$ phase. They have inferred that the transition from A_1 to $\tilde{C}$ occurs via the development of an intermediate smectic C phase with $\tilde{C}$ like polarization modulation fluctuations. The high resolution data also showed that the A_2 and C_2 phases have resolution limited peaks.

e) High Pressure Studies

We shall now discuss the results of our high pressure study on DB9.O.NO$_2$. The pressure-temperature (P-T) diagram of DB9.O.NO$_2$ showing all the phase boundaries (except the N-I phase boundary) is shown in Fig. 6.9. As mentioned erlier, owing to the limitations in the maximum working temperature of the high pressure cell, we did not monitor the N-I transition temperature as a function of pressure. The following features are seen from the P-T diagram.

i The A_d as well as the $A_{d(re)}$ phases are completely bounded in the P-T plane, the phase boundries being elliptic in shape similar to what is seen in other reentrant nematogens. The maximum pressure of smectic stability (P_m) is 1.10 kbar for the A_d phase and 0.29 kbar for the $A_{d(re)}$ phase.

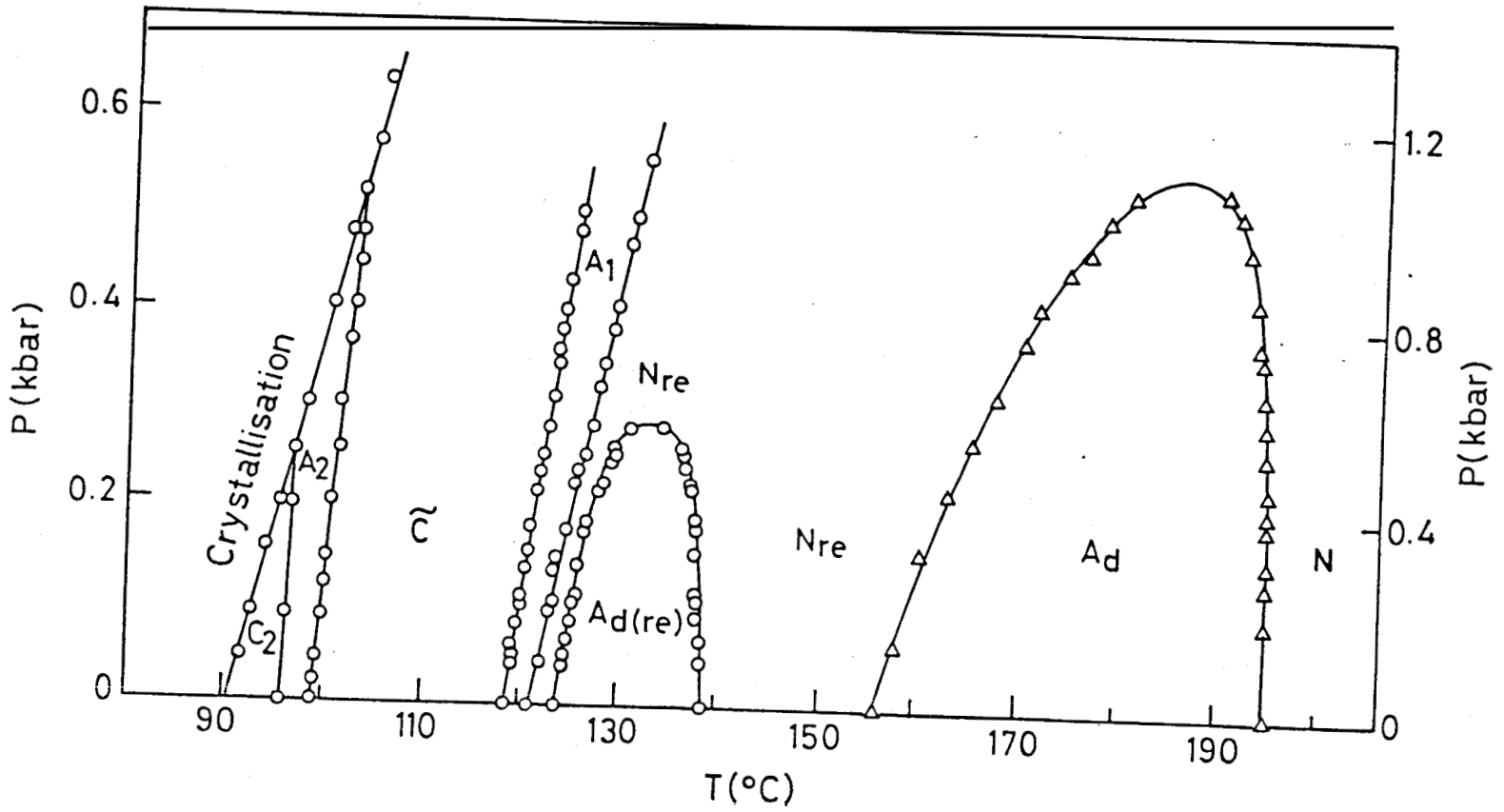

Figure 6.9

P-T diagram of DB9.O.NO_2. All transition temperatures were determined during the cooling mode. The pressure scale marked on the right-side is for data points shown as Δ.

ii The A_1-N_{re} phase boundary is straight throughout in contrast to the two A_d phases. This result which is similar to those observed earlier in other systems[21,22] indicates that the pressure behaviour of the A phase should be related to the extent of interdigitation of the molecules.

iii Both C_2 and A_2 phases are suppressed at high pressures because of the intersection of the crystallization line with the C_2 - A_2 and A_2 - $\tilde{C}$ phase boundaries respectively.

Thus the P–T diagram of DB9.0.NO_2 shows that both the A_d phases are unstable at high pressures. This diagram also shows dramatically that all the nematic phases the higher temperature normal nematic as well as the two reentrant nematic phases, are completely miscible at high pressure. Considering that it is difficult by Xray studies to distinguish the reentrant nematic phase with a strong smectic like ordering from the A_d phase, the pressure study is helpful in confirming the existence of three nematic phases at atmospheric pressure.

6.4.4. DB10.O.NO_2

Figure 6.10 shows the pressure – temperature diagram of DB10.O.NO_2. This P–T diagram is in several ways even more striking than that of DB9.O.NO_2 : we shall expand this further. The material exhibits only N, A_d, $\tilde{C}$ and C_2 phases at atmospheric pressure.

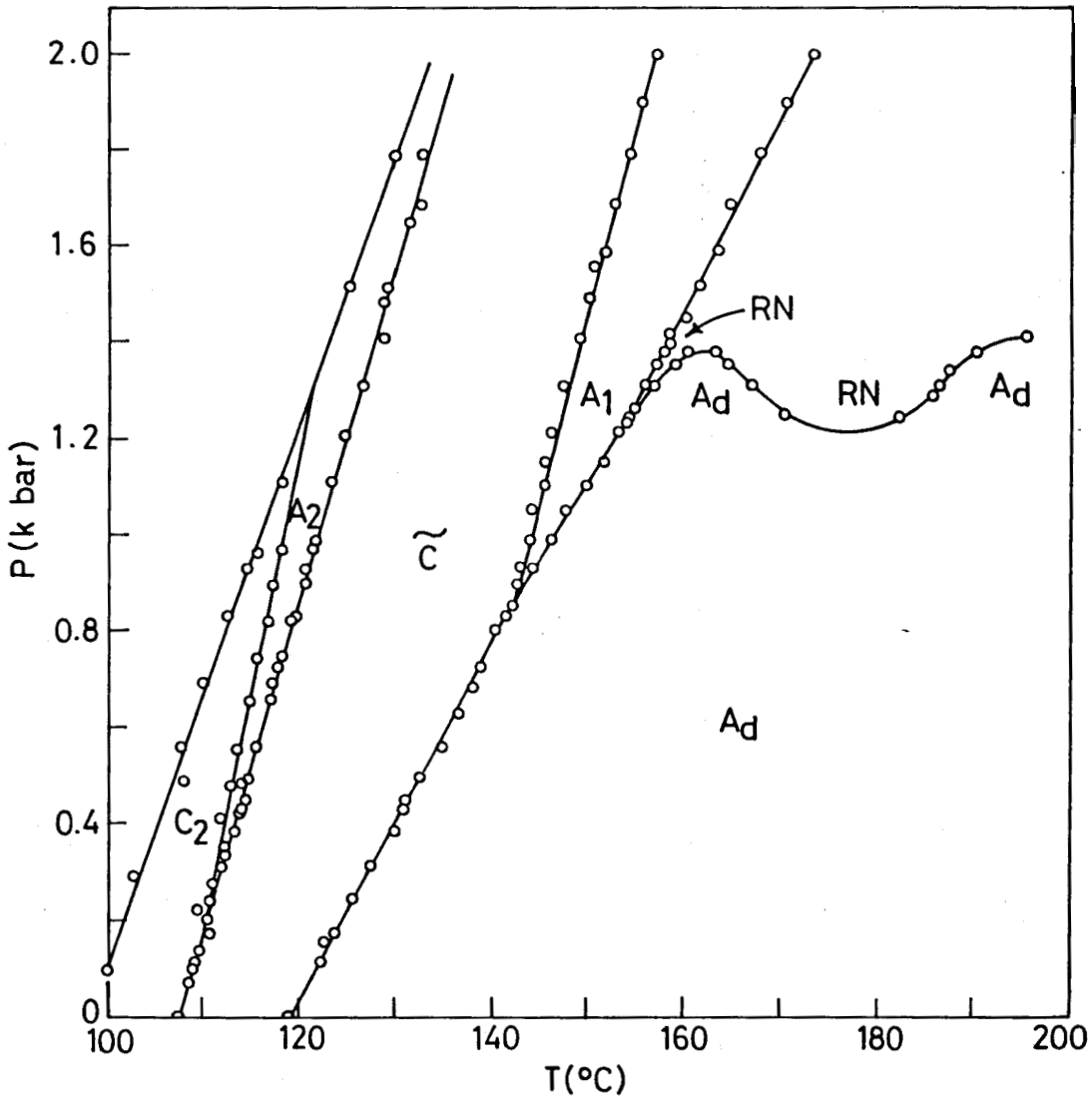

Figure 6.1 0

P-T diagram of DB10.O.NO_2.

However on increasing pressure several new phases are induced. The A_2 phase appears at a pressure of 0.2 kbar, the $C_2 - A_2$ boundary forking out of the $C_2 - \tilde{C}$ line. With increasing pressure the range of A_2 increases at the expense of C_2 until finally at about 1.25 kbar, the C_2 phase is suppressed. A second pressure induced phase (A_1) is seen beyond about 0.82 kbar, the $A_d - \tilde{C}$ boundary splitting into $\tilde{C} - A_1$ and $A_1 - A_d$ phase boundaries. [This phase has been identified as the A phase by optical observation of its texture at high pressure. A comparison of the phase diagram with the temperature-concentration diagram (Fig. 6.11) permits us to deduce that this phase is most likely to be the A_1 phase.] On further increase of pressure the $A_1 - A_d$ boundary forks out again - this time a nematic phase is induced - this is in fact the reentrant nematic phase. Finally perhaps the most dramatic part of the phase diagram is the appearance of two reentrant nematic phases seen in the pressure range of 1.26- 1.38 kbar. (It must be mentioned that owing to the limitations on the maximum temperature capability of the high pressure cell ($\geq$200°C) we could not study the $A_d - N$ or $N - I$ phase boundaries). In the pressure range 1.26 - 1.38 kbar, the following sequence of transitions are seen on decreasing temperature (at a constant pressure):

$$N \rightarrow A_d \rightarrow N_{re} \rightarrow A_{d(re)} \rightarrow N_{re} \rightarrow A_1 \rightarrow \tilde{C} \rightarrow A_2 \rightarrow C_2 \rightarrow K$$

This is nothing but the sequence of transitions seen in DB9.O.NO_2

at atmospheric pressure. Thus we have seen the first instance of a pressure-induced triply reentrant behaviour. It is also seen that the A_d phase gets bounded and shows a P_m of about 1.4 kbar. $A_{d(re)}$ also gets bounded and shows a P_m of about 1.39 kbar. The diagram also shows the existence of the $A_1 - N_{re} - A_d$ point. Although the topology of the diagram near this point is similar to the one seen for a bicritical point in a magnetic systems,[23] we could not ascertain the true nature of this point since it was not possible to conduct any high resolution study at such high pressures and temperatures. Also, as already remarked, the identification of A_1 phase is somewhat tentative and needs to be confirmed by X-ray studies at high pressure. If confirmed, the $A_1 - A_d$ transition seen in $DB10.O.NO_2$ at high pressure would be the first observation of such a transition in a single component liquid crystalline system.

Thus we have shown that $DB10.O.NO_2$ exhibits an unusually interesting pressure-temperature diagram. Over a narrow range of pressure all the transitions seen in $DB9.O.NO_2$ at atmospheric pressure are reproduced. Comparing this with the simple P-T diagrams of $DB7.O.NO_2$ and $DB8.O.NO_2$ it is clear that phase transitions at high pressure are extremely sensitive to the changes in molecular length.

6.4.5 Studies on mixtures of $DB10.O.NO_2$ and DB8.O.NO2

We have so far discussed the effect of pressure on phase

transitions in the different homologues of the $DBn.O.NO_2$ series. In this section we shall present the results of our studies on binary mixtures of $DB8.O.NO_2$ and $DB10.O.NO_2$.

Considering that $DB9.O.NO_2$ exhibits triply reentrant behaviour at atmospheric pressure while $DB8.O.NO_2$ as well as $DB10.O.NO_2$ show only one type of A–N transition, it is of interest to see the result of mixing $DB8.O.NO_2$ and $DB10.O.NO_2$. Fig. 6.11 shows the temperature-concentration (T-X) diagram of this binary system. It is seen that the A_d - N boundary curls twice towards the concentration axis leading to the multi-reentrant behaviour. Also, for a certain concentration range it shows a $A_d - A_1$ boundary. A_2 phase is induced and is found to be stable only for a certain concerntration range. Finally it is clear that over a concentration range of 48 mol % to 53 mol % the sequence of transition is exactly the same as that seen in $DB9.O.NO_2$ at atmospheric pressure(or in $DB10.O.NO_2$ over a region of pressure 1.26–1.38 kbar).

Finally, in order to see if we can induce, as we did in $DB10.O.NO_2$, a multi-reentrant behaviour in this system also, we have carried out a high pressure study of 57 mol % mixture of $DB10O.O.NO_2$ in $DB8.O.NO_2$. The pressure-temperature diagram of the mixture is shown in Fig. 6.12. The features of this diagram are:

1 the A–N boundry curls twice towards the pressure axis leading

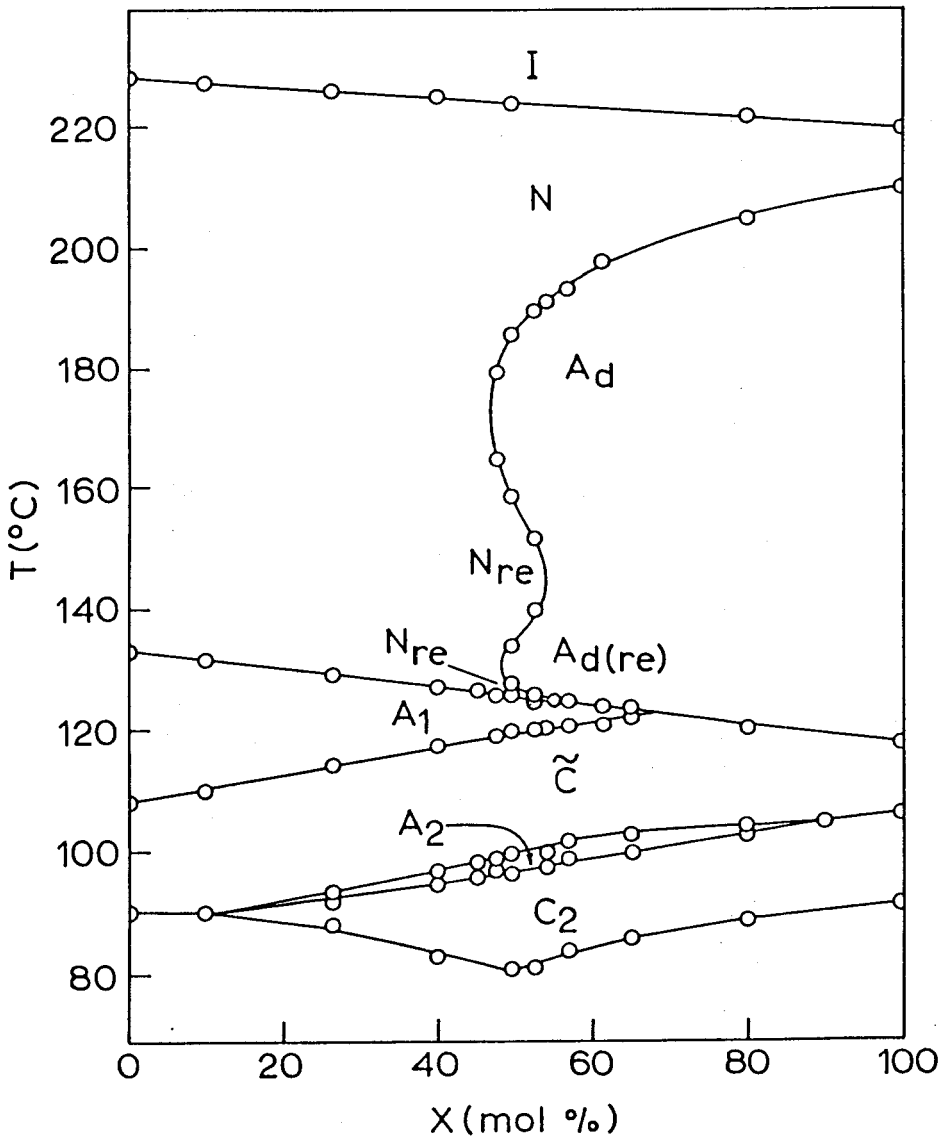

Figure 6.1 1

Temperature-concentration diagram (at 1 bar) for binary mixture of DB10.O.NO_2 and DB8.O.NO_2. X is the mol % of DB10.O.NO_2 in the mixture.

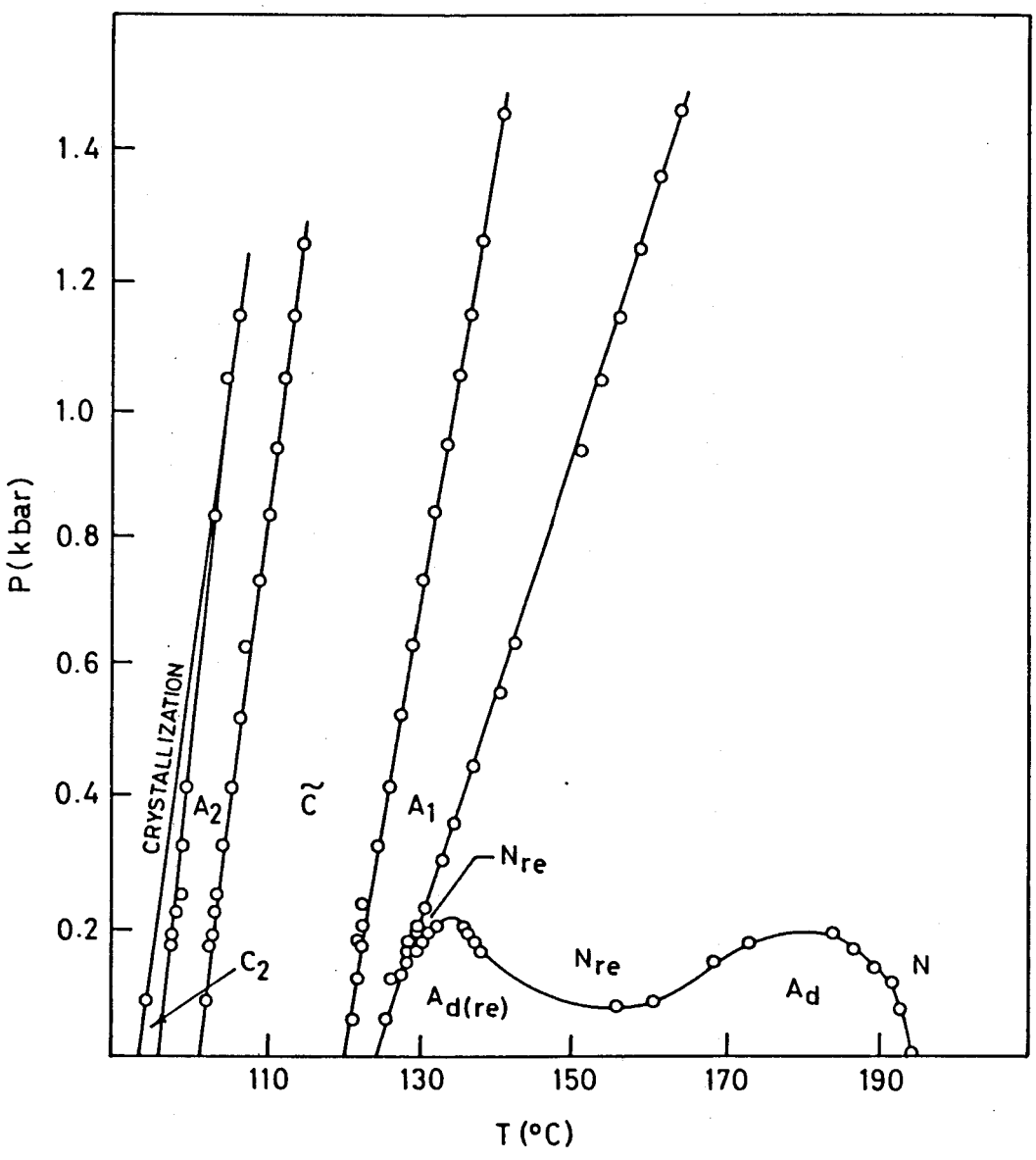

Figure 6.12

P-T diagram of X = 57 mol % DB10.O.NO$_2$ in DB8.O.NO$_2$.

to the multi-reentrant behaviour,

2 The A_d phase gets bounded showing a P_m of about 0.25 kbar while $A_{d(re)}$ gets bounded at 0.21 kbar,

3 $A_1 - N_{re} - A_d$ point is seen at 0.13 kbar,

4 The $A_1 - N_{re}$ boundary is linear throughout,

5 The C_2 phase gets suppressed under high pressure.

Thus the P-T diagram of 57% mixture of DB10.O.NO_2 and DB8.O.NO_2 is very similar to that of DB10.O.NO_2 except that all the features are now reproduced at lower pressures.

6.4.6 Comparison of experimental phasediagrams of DB9.O.NO_2 and DB10.O.NO_2 with the theoretical diagrams

A microscopic theory, known as the Frustrated Spin-Gas Model, has been developed[24-26] to explain the different reentrant sequences of nematic and smectic A phases, viz., $N - A_d - N$, $N - A_d - N - A_1$ and $N - A_d - N - A_d - N - A_1$. We shall summarise the most salient features of this theory in its present form.

A schematic representation of a pair of molecules of DB9.O.NO_2 (taken to be typical of reentrant mesogenic systems) is shown in Fig. 6.13. The rod shaped molecules are approximately 30 Å long and 5 Å thick. They have a longitudinal electric dipolar head,

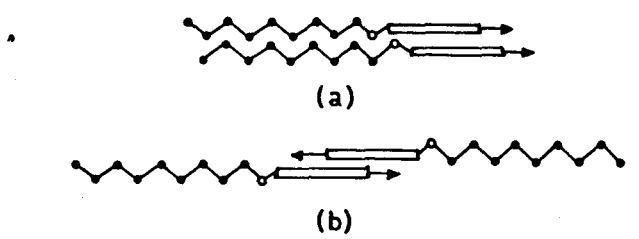

Figure 6.13

Schematic representation of molecules of the compound DB9.O.NO$_2$. Arrows denote dipolar heads, rectangles represent altomatic cores, open circles indicate oxygen atoms, and closed circles mark the positions of carbon atoms in all-trans configuration of the aliphatic tail. The molecular configurations of the pairs showing dominant (a) tail-tail attltaction, olt (b) steric hindrance are also shown.

a rigid aromatic core and a semi-flexible aliphatic tail. The spin-gas model embodies intermolecular hindrance, Van der Waals attraction and dipole-dipole forces, the last of these being most important. The neighbouring molecules are taken to interact via the pair potential,[24,27]

$$V(r_1,\hat{S}_1,r_2,\hat{S}_2) = [A\hat{S}_1.\hat{S}_2 - 3B(\hat{S}_1.\hat{r}_{12})(\hat{S}_2.\hat{r}_{12})]/|r_{12}|^3 , \qquad (1)$$

where r_i is the position of the dipole of molecule i, $\hat{S}_i$ is the unit vector describing the dipolar orientation, and $r_{12} = r_1 - r_2$ and $\hat{r}_{12} = r_{12}/|r_{12}|$. For purely dipolar forces, A = B. The alternative possibilities of dominant tail-tail attraction (Fig. 6.13a) or steric hindrance (Fig. 6.13b) are incorporated[24,27] in the ratio B/A : B < A for net hindrance (favouring the antiferroelectric term) and B > A for net entanglement (disfavouring the antiferroelectric term). Fluctuations towardsthe isotropic phase are ignored, namely, the molecules are taken aligned along the Z direction: $\hat{S}_i = \pm Z$, or simply $S_i = \pm 1$. Screening suppresses interactions between further neighbours. In the close-packing of a liquid, the potential in equation (1) inherently causes frustration due to substantial cancellations of forces between a molecule and its nearest neighbours (Fig. 6.14b,c).

The molecular tails play a crucial role. Apart from the free energy of their entanglement embodied in B/A, their lengthwise corrugation is essential, creating energetically preferred positions ("notches") of mutual permeation, i.e., positional fluctuation

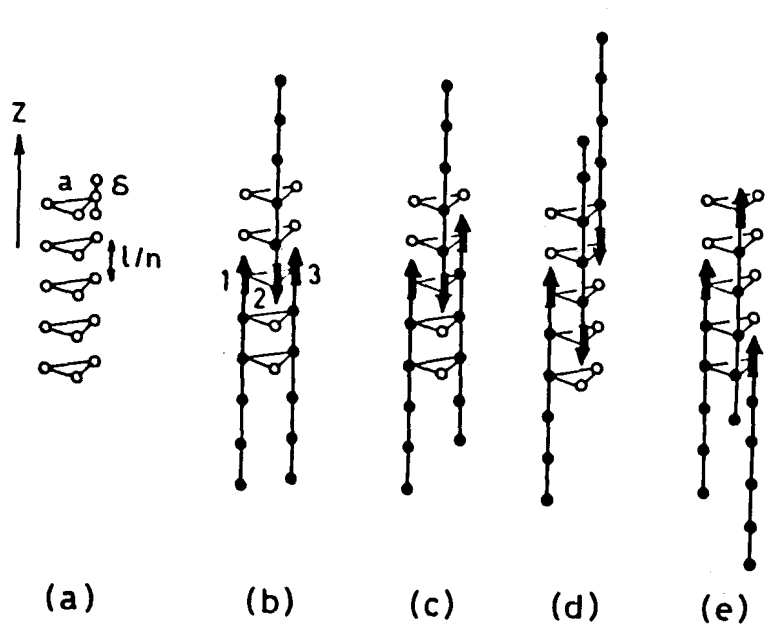

Figure 6.14

Schematic representation of configurations of a triplet of molecules. la) The atomic permeation positions of the dipole heads. Libzational permeation positions are illustrated only in the upper fight-hand corner. (b) A frustrated configuration: A zezo net force is felt by eithez of dipoles 1 and 3. (c) Anothelr frustrated configuration: A zero net force is felt by dipole 3. Configurations (b) and (c) are thus not conducive to layezing. On the othez hand, (d) and (e) are configurations in which frustrations is relieved by pezmeation, respectively conducive to inter-digitated paztial bilayer A_d *and the monolayer A, smectic spacing.*

along the Z-direction, for a nearest neighbour pair (see Fig. 6.14a). In addition to discrete "atomic" permeations on a length scale ℓ/n (a few $\mathring{A}$), where $4 \leq n \leq 8$, small oscillations are of course allowed on a subscale $m6 << \frac{\ell}{n}$. These "librational" permeations can be approximated to occur in m discrete subnotches within each notch.

Indekeu and Berker have obtained different theoretical phase diagrams for different values of B/A, n, m and δ. Figures 6.15a, 6.16a and 6.17a show the theoretical diagrams for two sets of values for B/A,n,m and 6. The first one, viz., Fig. 6.15a evidently resembles the pressure-tem er -ture diagram of 90BCAB reported[28] earlier (Fig. 6.15b). The theoretical diagram shown in Fig. 6.16a when considered for a/ℓ values < 0.466 is exactly similar to the pressure-temperature diagram of $DB9.0.NO_2$ (Fig. 6.16b). On the other hand the complete theoretical phase diagram (Fig. 6.17a) considered over the entire range of a/ℓ values is very similar to the diagram of $DB10.0.NO_2$ (see Fig. 6.17b).

Thus the spin gas model is able to reproduce satisfactorily all the features of the experimentally observed phase diagrams of reentrant and multi-reentrant systems. In fact the recent version of theory has predicted an even more exciting reentrant sequence, viz., $N - A_d - N - A_d - N - A_1 - N - A_d - N - A_1$. Such a sequence has not been observed experimentally.

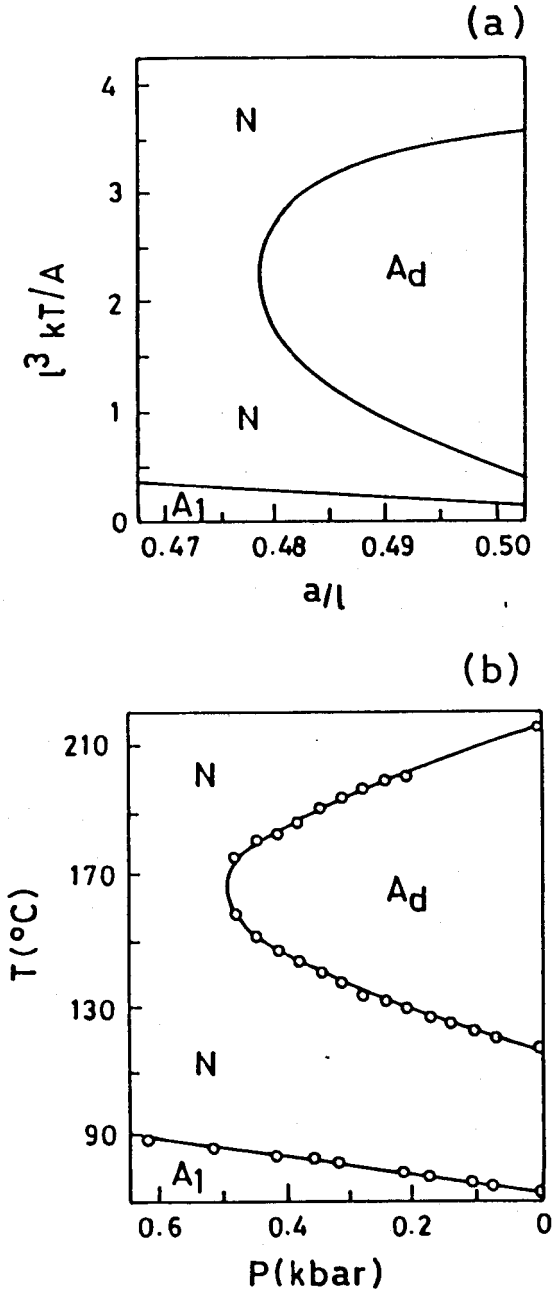

Figure 6.15

(a) *Doubly reentrant phase diagram obtained for* $\frac{B}{A} = 1.5$, $n = 5$, $m = 3$, *and* $6 = 0.01\ \frac{\ell}{n}$ *in the spin-gas model.*

(b) *Experimentally observed phase diagram for the compound 9OBCAB exhibiting the, doubly ieentrant phenomena. (From Ref. 28).*

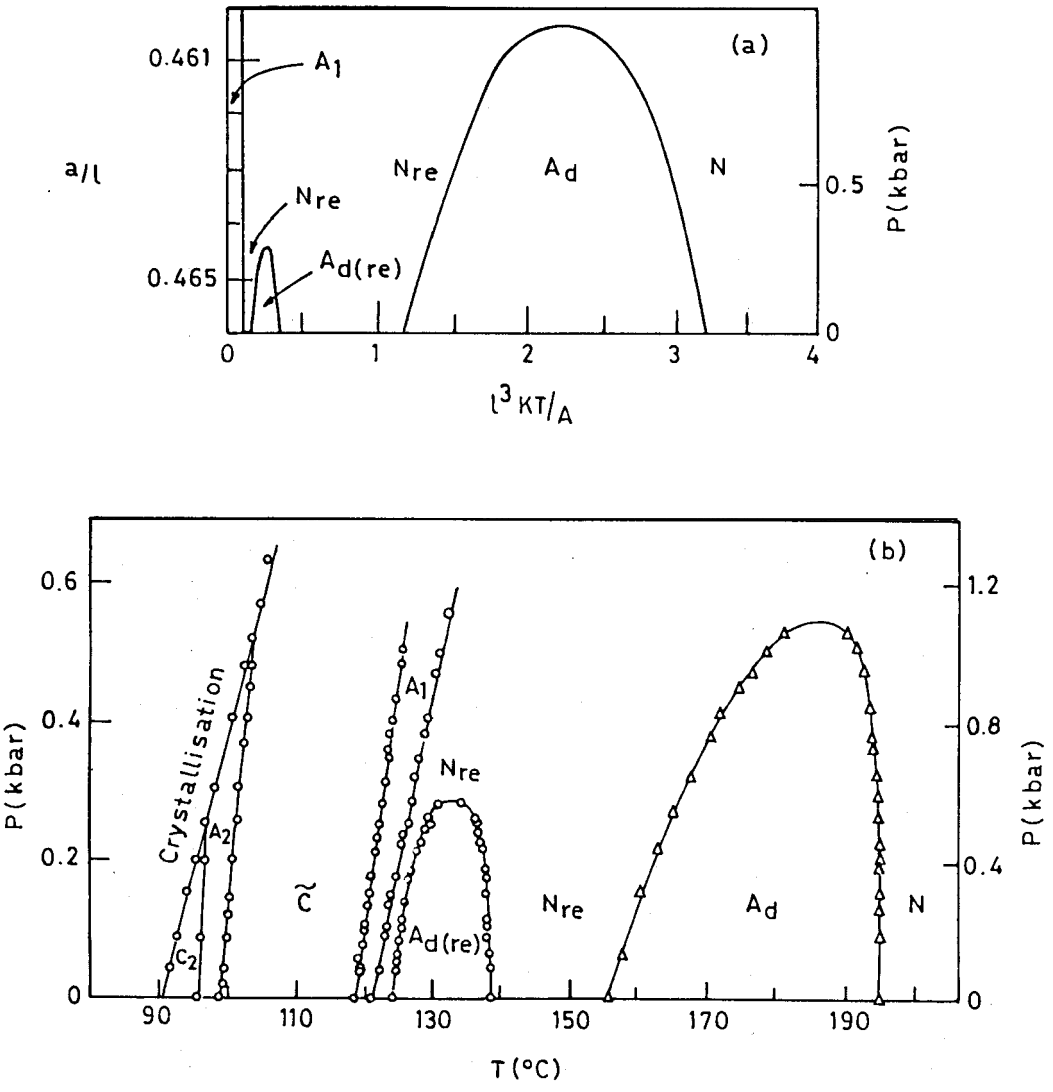

Figure 6.16

***Quadruply** reentrant phase **diagram obtained** for B/A = **1.455**, n = 5, **m** = 3, δ = 0.015 $\frac{\ell}{n}$. (a) A **tentative** pressure scale is **given** for **the** sake of comparison **with the experimentally observed** phase **diagram. (From** Ref. **26).** (b) Experimental P-T diagram of DB9.O.NO_2 **exhibiting quadruple** reentrance.*

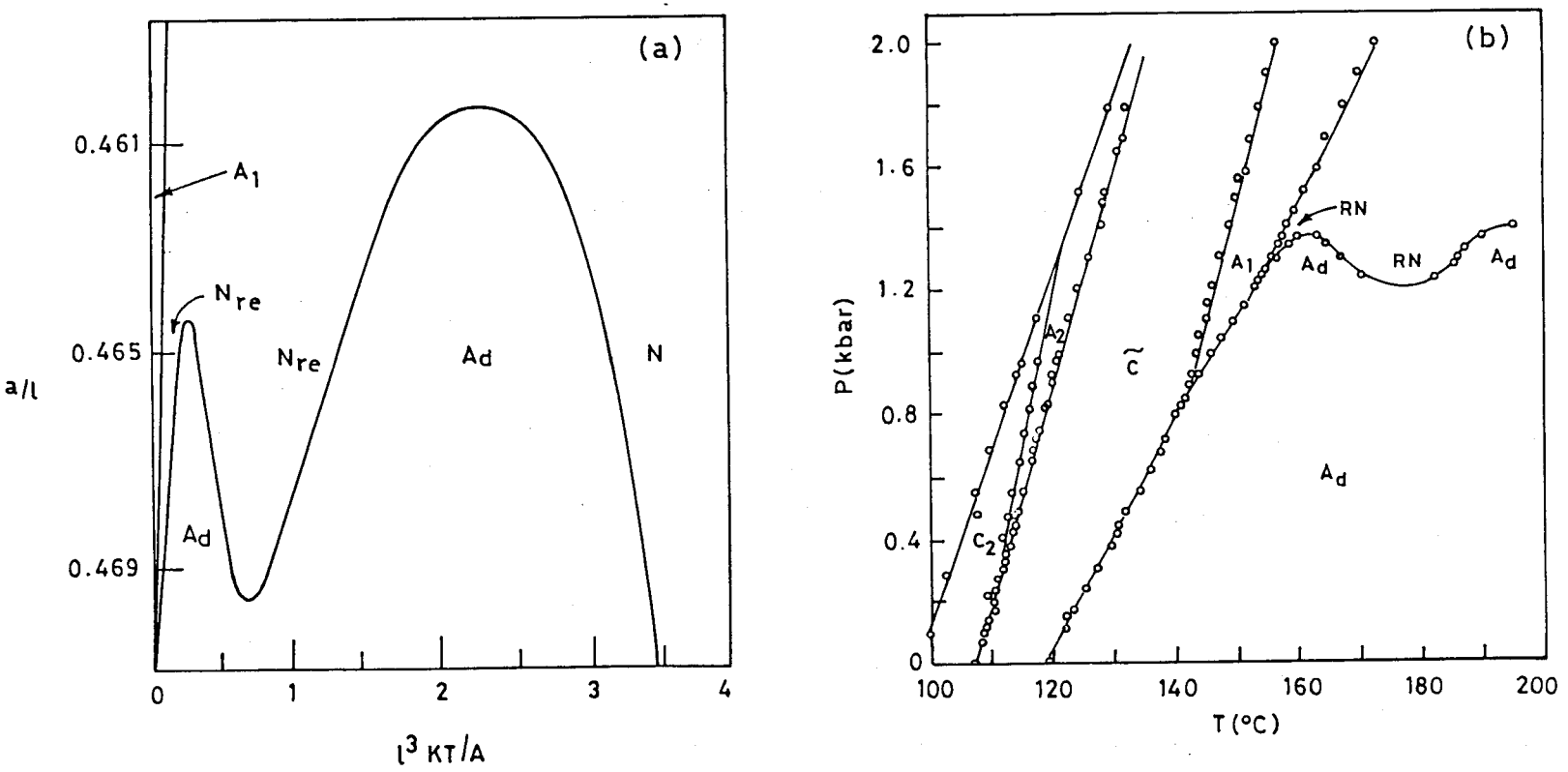

Figure 6.17

Quadruple reentrant phase diagram obtained for $\frac{B}{A} = 1.455$, $n = 5$, $m = 3$, *and* $\delta = 0.015\frac{\ell}{n}$. *(a) theoretical diagram considered over the entire range of* a/ℓ *(From Ref. 26) is rotated by 90° for the sake of comparison with the experimental observed diagram. (b) P-T diagram DB10.O.*NO_2 *exhibiting the quadruple reentrants.*

REFERENCES

1 P.E.Cladis, Phys. Rev. Lett., 35, 48 (1975)

2 A.C.Anderson, W.Reese and J.C.Wheatly, Phys. Rev., 130, 1644 (1963)

3 G.Riblet and K.Winzer, Solid State Commun., 9, 1663 (1971)

4 B.T.Mathias, E.Corenwit, J.M.Vandenberg and H.E.Barz, Natl. Acad. Sci. (USA), 74, 1334 (1977)

5 V.T.Rajan and C.W.Woo, Phys. Lett., **73A**, 224 (1979)

6 P.E.Cladis, R.K.Bogardus, W.B.Daniels and G.N.Taylor, Phys. Rev. Lett., 39, 720 (1977)

7 F.Hardouin, G.Sigaud, M.F.Achard and H.Gasparoux, Phys. Lett., **71A**, 347 (1979)

8 N.V.Madhusudana, B.K.Sadashiva and K.P.L.Moodithaya, Curr. Sci., 48, 613 (1979)

9 G.Heppke, R.Hopf, B.Kohne and K.Praefcke, Proc. Third Liq. Cryst. Conf. of Socialist Countries, Budapest, 1979, Ed. L. Bata(Pergamon, Oxford, 1980), p. 141.

10 A.M.Levelut, F.Hardouin and G.Sigaud, Proc. Intern. Liquid Cryst. Conf., Bangalore, 1979, Ed. S.Chandrasekhar (Heyden, London, 1980), p. 143; F.Hardouin and A.M.Levelut, J. de Phys., 41, 41 (1980)

11 K.A.Suresh, R.Shashidhar, G.Heppke and R. Hopf, Mol. Cryst. Liq. Cryst., 99, 249 (1983).

12 Nguyen Huu Tinh, J. Chim. Phys., 80, 83 (1983)

13 G.Pelzl, S. Diele, I. Latif, W.Weissflog and D.Demus, Cryst. Res. Technol., 17, K78 (1982)

14 Nguyen Huu Tinh, F.Hardouin and C.Destrade, J. de Phys., 43, 1127 (1982)

15 G.W.Gray and J.W.Goodby, Smectic Liquid Crystals - Textures and Structures, (Leonard Hill, 1984), p. 146.

16 F.Hardouin, A.M.Levelut, M.F.Achard and G.Sigaud, J. Chim. Phys., 80, 53 (1983)

17 F. Hardouin and A.M.Levelut, J. de Phys., 41, 41 (1980)

18 J. Wang and T.C.Lubensky, J. de Phys., 45, 1653 (1984)

19 F.Hardouin, Nguyen Huu Tinh, M.F.Achard and A.M. Levelut, J. de Phys. Lett., 43, L-327 (1982)

20 E.Fontes, P.A.Heiney, John N. Hareltine and Amos B. Smith III, J. de Phys., 47, 1533 (1986)

21 P.E.Cladis, in "Liquid Crystals", Proc. Int. Conf., Bangalore, December 1979, Ed. S. Chandrasekhar (Heyden, London, 1980), p. 105

22 S.Krishna Prasad, R.Shashidhar, A.N.Kalkura, K.A. Suresh, G. Heppke and R. Hopf, Mol. Cryst. Liq. Cryst., 99, 185 (1983)

23 Y.Shapira, in "Multicritical Phenomena", Ed. R. Pynn and A. Skjeltrop (Plenum, New York and London, 1983), p. 35.

24 A.N.Berker and J.W.Walker, Phys. Rev. Lett., 47, 1469 (1981)

25 J.O.Indekeu and A.N.Berker, Physica, A 140, 368 (1986)

26 J.O.Indekeu and A.N.Berker, J. de Phys., 49, 353 (1988)

27 J.O.Indekeu and A.N.Berker, Phys. Rev., A 33, 1158 (1986)

28 R.Shashidhar, B.R.Ratna and S. Krishna Prasad, Mol. Cryst. Liq. Cryst., 130, 179 (1985)